Chapter 13
Titania–Montmorillonite for the Photocatalytic Removal of Contaminants from Water: Adsorb & Shuttle Process

Ridha Djellabi, Mohamed Fouzi Ghorab, Abdelaziz Smara, Claudia Letizia Bianchi, Giuseppina Cerrato, Xu Zhao, and Bo Yang

Contents

R. Djellabi (✉)
Research Center for Eco-Environmental Sciences, Chinese Academy of Sciences, Beijing, People's Republic of China

Department of Environmental Engineering, College of Chemistry and Environmental Engineering, Shenzhen University, Shenzhen, People's Republic of China

Laboratory of Water Treatment and Valorization of Industrial Wastes, Chemistry Department, Faculty of Sciences, Badji-Mokhtar University, Annaba, Algeria

M. Fouzi Ghorab · A. Smara
Laboratory of Water Treatment and Valorization of Industrial Wastes, Chemistry Department, Faculty of Sciences, Badji-Mokhtar University, Annaba, Algeria

C. L. Bianchi
Università degli Studi di Milano, Dip. Chimica and INSTM-UdR Milano, Milan, Italy

G. Cerrato
Università degli Studi di Torino, Dipartimento di Chimica and NIS Interdepartmental Centre and Consorzio INSTM-UdR, Torino, Italy

X. Zhao
Research Center for Eco-Environmental Sciences, Chinese Academy of Sciences, Beijing, People's Republic of China

B. Yang
Department of Environmental Engineering, College of Chemistry and Environmental Engineering, Shenzhen University, Shenzhen, People's Republic of China

M. Naushad, E. Lichtfouse (eds.), *Green Materials for Wastewater Treatment*, Environmental Chemistry for a Sustainable World 38,
https://doi.org/10.1007/978-3-030-17724-9_13

Abstract Recently, TiO_2–Montmorillonite-based composites have attracted a great deal of attention as efficient photocatalysts for the degradation/reduction of organic contaminants and heavy metals in waters and wastewaters. It can be claimed that the most popular benefits of using TiO_2–Montmorillonite photocatalysts are an enhancement in the photocatalytic removal of contaminants due to their high adsorption capacity, high photocatalytic activity of nanoscaled TiO_2 deposited on Montmorillonite surface and low costs. Otherwise, the use of naked nanoscaled TiO_2 is not recommended because of its low adsorption ability, fast agglomeration in water and due to the issue of recovery of such small particles from water. Differently from naked TiO_2, the photocatalytic removal of contaminants by TiO_2–Montmorillonite is enhanced through the mechanism so-called Adsorb & Shuttle (A&S) which is based on the use of highly adsorbing domains to increase the quantity of contaminants near TiO_2 photocatalytic sites. Adsorb & Shuttle process can be affected by TiO_2–Montmorillonite characteristics (i.e. TiO_2 loading, surface area, pore size and degree of TiO_2 crystallinity) as well as the type of contaminant. In this chapter, the following points will be highlighted: (i) mechanisms of TiO_2 photocatalysis for the removal of organic contaminants and heavy metals, (ii) recent progress on synthesis of TiO_2–Montmorillonite photocatalysts via different methods and (iii) recent discussions regarding the photocatalytic removal of contaminants by TiO_2–Montmorillonite composites.

Keywords TiO_2–Montmorillonite · Photocatalysis · Adsorb & Shuttle · Water remediation · Organic contaminants · Heavy metals

13.1 Introduction

Due to the dramatic increase in population growth and agricultural and industrialization activities, water demand has increased up to ninefold in the twentieth century (Shenvi et al. 2015). Many countries are expected to face water crisis in the next decades. Thereby, water purification and reuse have become one of the major global concerns in scientific community. Researchers are developing water purification technologies that might be environmentally friendly, economical, and efficient. Among these technologies, the photocatalysis has been considered as one of the most efficient and low-cost processes for water decontamination (Malato et al. 2009; Zheng et al. 2013; Shenvi et al. 2015; Zhang et al. 2018). Titanium dioxide has been extensively in environmental remediation due to its desirable photocatalytic activity, high photostability, non-toxicity, low cost and biocompatibility (Hashimoto et al. 2005; Nakata and Fujishima 2012; Fagan et al. 2016; Waqas et al. 2017). The photocatalysis process is focused on the absorption of UV light by TiO_2 leading to photoexcite the electrons from the valence band to conduction band; therefore, electron/hole pair charges will be formed at the surface of TiO_2. Organic pollutants can be directly degraded by positive holes at the valence band or by the

produced hydroxyl radicals via H_2O/positive holes reaction, while the reduction of heavy metals to lower/higher metallic states occurs at the conduction band of TiO_2 by the photogenerated electrons in the presence of hole scavenger molecules (Lee and Park 2013, Lu 2013, Djellabi et al. 2014, Djellabi and Ghorab 2015a, b, Litter 2015, Djellabi et al. 2016a, b, c, Djellabi et al. 2017, Litter 2017, Marinho et al. 2018).

One of the major obstacles facing the implementation of photocatalysis stems from the fact that the photocatalytic removal of pollutants from water depends on adsorption rate of pollutants on the photocatalyst surface. Therefore, it is difficult to photodecompose many hazardous pollutants that hardly adsorb on TiO_2 surface, due to poor affinity of TiO_2 for hydrophobic organic substances. Additionally, industrial wastewaters usually contain several organic and inorganic pollutants which compete for the adsorption sites of the TiO_2 surface, thus inhibiting the efficiency of the process. On the other hand, the photo-oxidation of single organic pollutant can produce many harmful by-products/intermediates that could not be adsorbed on TiO_2 surface for further degradation. It is worth noting that, in practice, the use of nanoscale TiO_2 particles is not recommended due to the issue of recovery of such fine particles from water, and also these nanoscale particles are prone to agglomerate in water limiting the photoactivity. In order to overcome drawbacks of commercial TiO_2, many offers have been made to design new composite photocatalysts via several strategies including metal/non-metal doping, sensitization and coupling of semiconductors. In particular, the combination of TiO_2 nanoparticles with porous adsorbent materials has been proved to be a successful strategy for enhancing the photocatalytic efficiency as reported by several authors (Bhattacharyya et al. 2004; Romero et al. 2006; Zou et al. 2006; Yahiro et al. 2007; Mahalakshmi et al. 2009; Yang et al. 2009; Zhang et al. 2009; Manova et al. 2010; Yu et al. 2012; Vicente et al. 2013; Djellabi et al. 2014; Du and Zheng 2014; Wang et al. 2014; Belver et al. 2015; Yang et al. 2015; Belver et al. 2016; López-Muñoz et al. 2016; Belver et al. 2017; Gebru and Das 2017; Petronella et al. 2017; Srikanth et al. 2017; MiarAlipour et al. 2018). Among these minerals, Montmorillonite has been widely used. Montmorillonite contains layered structure and exhibits very high porosity and high external and internal surface area and large CE capacity which allow the adsorption of organic or metallic pollutants via electrostatic of ion exchange within its interlaminar spaces (Kameshima et al. 2009a; Chen et al. 2012). It is important to point out that the introduction of TiO_2 nanoparticles into layered Montmorillonite enhances the photocatalytic activity due to synergistic effects resulting from the combination of adsorbent and TiO_2. On the other hand, the Montmorillonite can stabilize TiO_2 nanoparticles and increase the concentration of pollutants into the surface of the composite leading to facilitate their degradation/reduction by the photoactive TiO_2 particles. Certain aspects regarding the recent progress on synthesis and application of TiO_2–Montmorillonite for water remediation will be highlighted in the chapter.

13.2 Mechanism of TiO_2 Photocatalysis for Water Treatment

The photonic and mechanistic pathways underlying the phenomenon of TiO_2 photocatalysis for water/air remediation have been extensively investigated and reported (Herrmann 1999; Fujishima et al. 2000; Rauf and Ashraf 2009; Byrne et al. 2017). Photocatalysis is a green strategy that can be employed for environment remediation and energy production using semiconductor photocatalysts under light irradiation. As above-mentioned, titanium dioxide semiconductor (TiO_2) has been largely applied because of its special physical and photonic characteristics. When TiO_2 surface is irradiated by photon energy ($h\upsilon$) of higher than or equal to TiO_2 band gap energy, which is known to be 3.2 eV (anatase) or 3.0 eV (rutile), photo-induced electrons/positive holes changes will be formed at the surface of TiO_2 via the excitation of electrons from the valence band (VB) to conduction band (CB) in femtoseconds. Figure 13.1 illustrates the possible pathways for the production of electron/hole pairs on TiO_2 particle. For TiO_2 case, usually, the photonic excitation requests a light wavelength < 400 nm. A positively charged empty valence band will be produced when the electron moves to the conduction band. Different redox reactions occur at the surface of photoexcited TiO_2 which are responsible for the oxidation and reduction of pollutants and widely reported as follows:

$$\text{Photonic excitation of } TiO_2 : TiO_2 + h\upsilon \rightarrow e^- + h^+ \tag{13.1}$$

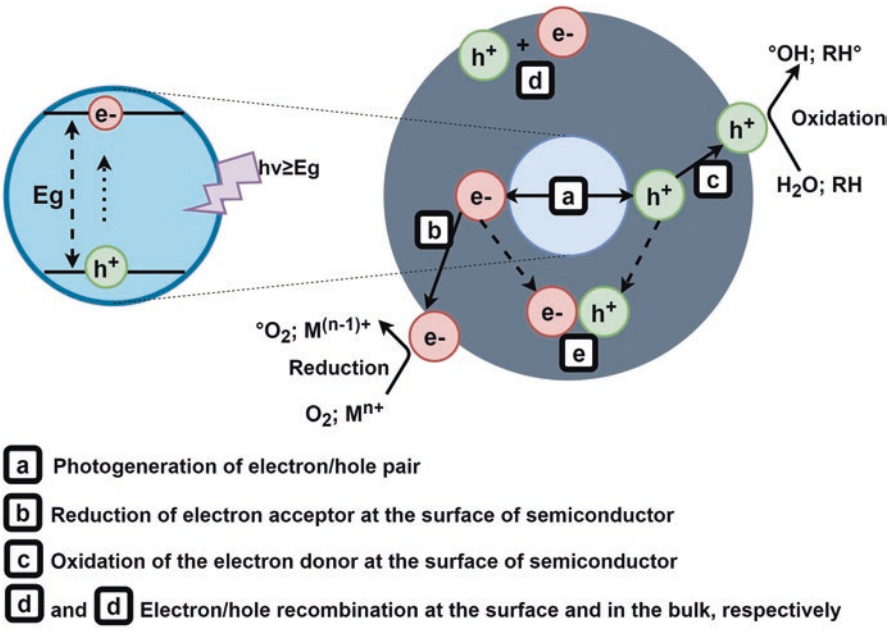

Fig. 13.1 Mechanistic pathways occurring at the photoexcited semiconductor particle

$$\text{Trapping of electrons}: e_{CB}^{-} \rightarrow e_{TR}^{-} \tag{13.2}$$

$$\text{Trapping of positive holes}: h_{VB}^{+} \rightarrow h_{TR}^{+} \tag{13.3}$$

$$\text{Recombination of charges}: e_{TR}^{-} + h_{VB}^{+}\left(h_{TR}^{+}\right) \rightarrow e_{CB}^{-} + \text{heat} \tag{13.4}$$

$$\text{Scavenging of electrons}: \left(O_2\right)_{ads} + e^{-} \rightarrow O_2^{\circ -} \tag{13.5}$$

$$\text{Photoreduction of metallic cations by } e^{-}: M^{n+} + e_{CB}^{-} \rightarrow M^{(n-1)+} \tag{13.6}$$

$$\text{Production of hydroxyl radicals}: OH^{-} + h^{+} \rightarrow {}^{\circ}OH \tag{13.7}$$

$$\text{Oxidation of organics by } {}^{\circ}OH: R - H + OH^{\circ} \rightarrow R^{\circ} + H_2O \tag{13.8}$$

$$\text{Oxidation of organics by } h^{+}: RH + h^{+} \rightarrow R^{+\circ} \rightarrow \text{Intermediate}(s) / \text{Final products} \tag{13.9}$$

$$\text{Protonation of superoxides}: O_2^{\circ -} + {}^{\circ}OH \rightarrow HOO^{\circ} \tag{13.10}$$

$$\text{Co} - \text{scavenging of } e^{-}: HOO^{\circ} + e^{-} \rightarrow HO_2^{-} \tag{13.11}$$

$$\text{Production of } H_2O_2: HOO^{-} + H^{+} \rightarrow H_2O_2 \tag{13.12}$$

e_{TR}^{-} and h_{TR}^{+}in (Eq. 13.4) show the trapping of electrons at the conduction and the holes at the valence band, respectively. It is important to note that the trapping of charges takes place at the surface of the semiconductor, while their recombination does not occur immediately after the photonic excitation (Fujishima et al. 2000). Without the presence of electron scavengers such as oxygen in the medium, the photogenerated electrons can easily recombine with the positive holes accompanying with dissipation of heat energy. Therefore, in order to carry out the photocatalysis action, the presence of electrons acceptor is imperative to avoid the quick electron/hole recombination (enhanced separation of charges ensures an efficient photocatalytic reaction). As shown in Eq. 13.5, the presence of oxygen molecules inhibits the combination of electron/hole pair charges; therefore, the production of superoxides radical $^{\bullet}O_2^{-}$ takes place. Afterwards, $^{\bullet}O_2^{-}$ species can be further protonated to produce the hydroperoxyl radical HOO$^{\bullet}$ and then H_2O_2 as indicated in Eqs. 13.10, 13.11 and 13.12. It was reported that HOO$^{\bullet}$ species may also play the role of electrons scavenging at the conduction band which enhances the separation charges. It was deduced that all photocatalytic pathways occur because of the presence of both dissolved oxygen (DO) and water molecules to balance the redox reactions at the surface of the semiconductor. In the absence of water, the highly reactive hydroxyl radicals ($^{\bullet}$OH) can not be produced by the positive holes which limits the oxidation of organic pollutants. Some researchers have reported that the degradation of organics by photocatalytic action does not take place without H_2O

molecules. However, Byrne and Eggins reported that some small organic molecules (e.g., oxalate and formic acid) can be oxidized by photocatalytic system without water (Byrne and Eggins 1998).

While h^{+}_{TR} has been extensively considered to be a powerful oxidant (+1.0 to +3.5 V against NHE) for the degradation of organic species directly without hydroxyl radicals formation step, this pathway is still quite inconclusive. However, e^{-}_{TR} is known to be a good reductant (+0.5 to −1.5 V against NHE), which depends on the kind of the semiconductor as well as the reaction condition. Because the photocatalytic oxidation and reduction pathways take place mainly at the surface of the photoexcited semiconductor, the comprehension of the involved steps during the oxidation of organic pollutants is very important in the formulation of kinetic expression. Overall, the degradation of organics usually includes the formation by-products (intermediates) and further mineralized to CO_2 and H_2O as shown in (Eq. 13.13).

$$\text{Organic contaminants} \xrightarrow{TiO_2/h\upsilon} \text{Intermediate}(s) \rightarrow CO_2 + H_2O + \text{mineral salts} \tag{13.13}$$

Therefore, photocatalysis reaction can be divided into five steps as reported by Fogler and Herrmann (Fogler 2006; Herrmann 1999), as schematically revealed in Fig. 13.2:

1. Transfer of the pollutant species form the solution to the surface of the semiconductor.
2. Pollutant species adsorption into the surface of the photoexcited semiconductor.
3. The photocatalytic reaction takes place for the adsorbed phase at the surface of the photoexcited semiconductor (oxidation of organics and reduction of heavy metals).
4. Desorption of the organics by-products or metallic/metal species from the surface of the semiconductor.
5. Mass transfer of the intermediate(s) from the interface domain to the bulk solution. However, by-products could also be adsorbed on the photocatalyst surface.

Beside the oxidation of organics by photocatalytic action, photocatalytic removal of metal ions from solution by different photocatalysts has attracted much attention recently. The reduction of several metallic cations was investigated and reported in the literature which includes Ag^{+}, Au^{3+}, Cd^{2+}, Cr^{6+}, Cu^{2+}, Fe^{3+}, Hg^{2+}, Ni^{2+}, Pb^{2+}, Pt^{4+}, Rh^{3+}, Tl^{+}, U^{6+}, Zn^{2+} and As^{3+}(Litter 1999; Kajitvichyanukul et al. 2002; Ruvarac-Bugarčić et al. 2005; Cristante et al. 2006; Kabra et al. 2008; Murruni et al. 2008; Williams et al. 2008; Litter 2009; López-Muñoz et al. 2009; Rodríguez et al. 2010; Lenzi et al. 2011; Singh and Chaudhary 2013; Mahlamvana and Kriek 2014; Mohamed and Salam 2014; Mahlamvana and Kriek 2015; Anggraini et al. 2016; Saien et al. 2016; Guo et al. 2017; Lee et al. 2017; Fontana et al. 2018; Marinho et al. 2018). It is important to note that the photocatalytic ability of a semiconductor such as TiO_2 for the reduction of metal cation can be obtained usually from the correlations of the metal cation redox potentials relative to the TiO_2 conduction band edge, as shown in Fig. 13.3. Many researchers have reported that these potentials can be

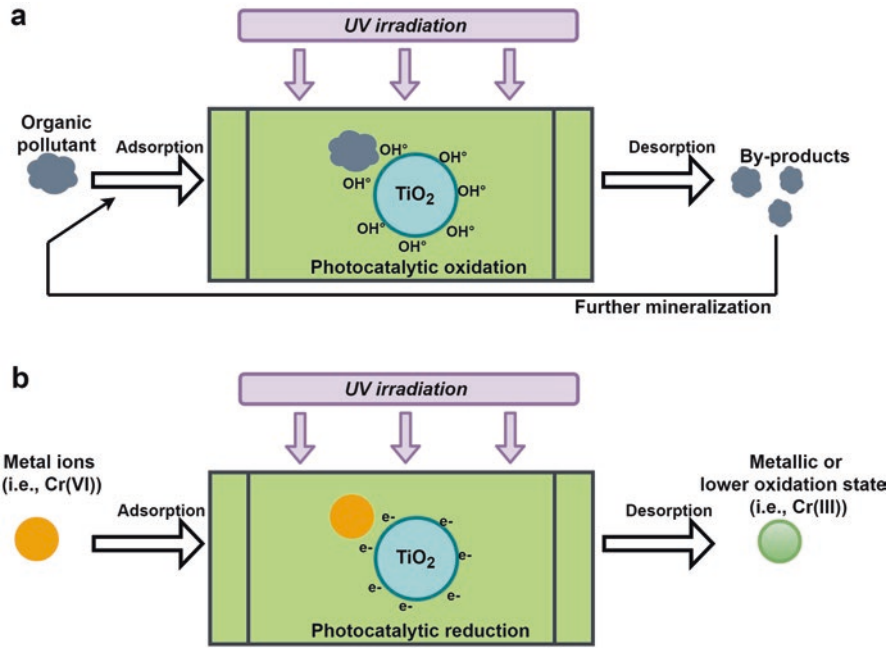

Fig. 13.2 Steps in heterogeneous photocatalytic reaction. (**a**) Oxidation of organic pollutants, (**b**) reduction of metal cations

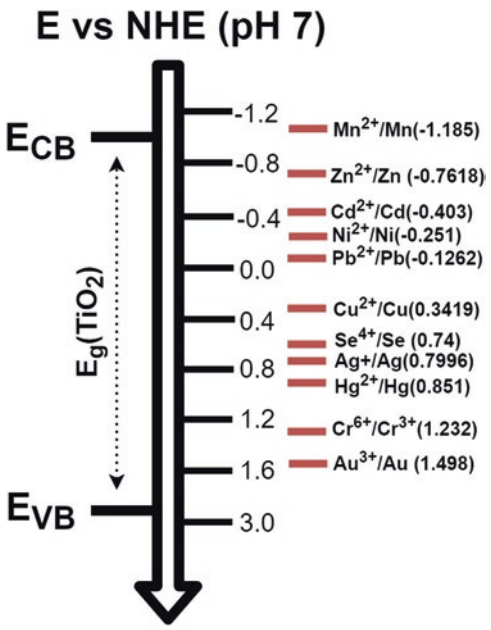

Fig. 13.3 Positions of CB and VB edges of TiO_2 relative to the standard potentials of several redox couples

shifted by pH or by solution conditions such as the concentration of species and the presence of co-adsorbates. The deposition of produced metal species after the photoreduction reaction on the photocatalyst surface can take place (Djellabi et al. 2016a, b, c). Moreover, in order to ensure an efficient reduction of metal cations, the addition of hole scavenger molecules (sacrificial electron donor) to the solution is very important. The oxidation of organic molecules on the photocatalyst surface allows the separation of electrons for metal cation reduction, as well as inhibits the reoxidation of metal cation. Furthermore, the choice of the hole scavenger molecule (usually a small organic molecule) is a key parameter, since the efficiency of metal cation reduction depends on the balancing oxidation reaction (Tan et al. 2003; Djellabi and Ghorab 2015a, b; Djellabi et al. 2016a, b, c). In addition, several groups have reported that the coordinated ligands to a metal cation such as EDTA can play the role of hole scavenger for the photocatalytic reduction of metal cations.

The mechanisms of metal cations photoreduction by TiO_2 can occur by direct or indirect reduction pathways (Fig. 13.4). The direct reduction takes place via the photogenerated electrons at the CB of the photocatalyst, in which, the conduction band edge of the photocatalyst must be more negative that the $M^{n+}/M^{(n-1)+}$ redox potential. When the metal cation valance charges are higher than 1 (i.e. Cr(VI)), single-electron transfer versus multiple-electron transfer pathways are still not clear. Testa et al. (Testa et al. 2001; Testa et al. 2004) have reported that, via EPR analysis, the single-electron transfer can take place for the photoreduction of Cr(VI) by photocatalysis, in which the reduction of Cr(VI) to Cr(III) passes by the formation of metastable Cr(V). While most researchers envision the direct transfer from CB of TiO_2 to metal cation, some groups (Marinho et al. 2017) have reported that indirect reduction of metal cation could also be possible. They suggested that species, such

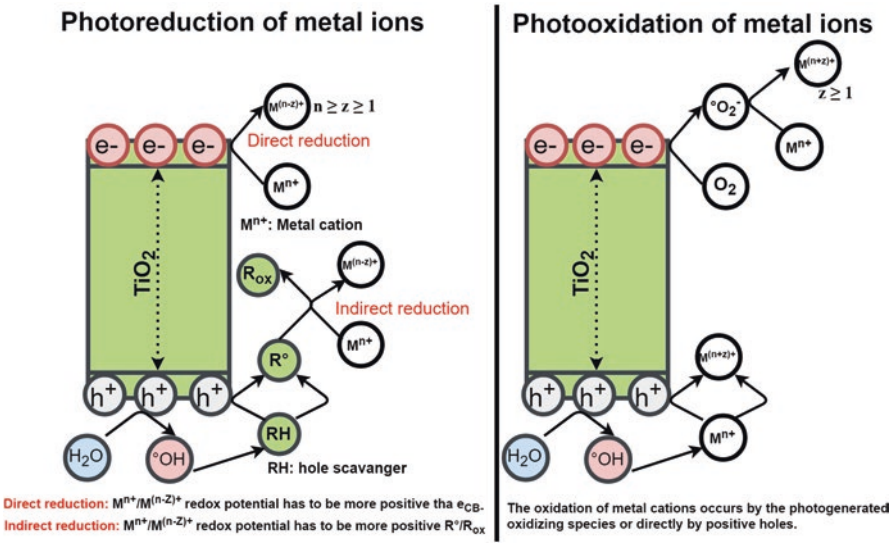

Fig. 13.4 Pathways of photocatalytic reduction and oxidation of metal ions on TiO_2

as $CO_2^{\bullet-}$ ($E_0(CO_2/ CO_2^{\bullet-}) \approx -2.0$ V), produced through the oxidation of electron donor molecules (hole scavengers) can reduce some metal cations. It is claimed that the indirect electron transfer system occurs independently of the redox potential of the metal ions. Additionally, the oxidation of metal cations, which can reach a higher oxidation state such as As(III) to As(V), can also occurred by the photogenerated oxidizing species or directly by positive holes at the conduction band (Fig. 13.4).

13.3 TiO_2–Montmorillonite-Based Composites

Aluminosilicate clay minerals have been widely used as adsorbents and to immobilize TiO_2 nanoparticles for water and wastewater purification. They are inexpensive, abundantly available and non-toxic and have good sorption properties and ion-exchange potential for pollutants (Özcan et al. 2005). They possess a wide pore size distribution, ranging from micro- (<20 Å) to mesopores (20–500 Å). The high porosity of these minerals is produced from fractures in the particle surfaces, staggered layer edges, whereas spaces are generated by overlapping of stacked layers and interlayer areas (Rutherford et al. 1997). The incorporation of various species and nanoparticles into the interlayer space allows aluminosilicates to be utilized as new functional materials (Yariv 2002). The basic structure of aluminosilicate minerals consists of a tetrahedral sheet of polymerized silica and octahedral sheet of alumina. The alumina octahedra can polymerize in two dimensions by sharing four O atoms, in which two oxygen atoms are left unshared, providing a 2- negative charge. This negative charge is counterbalanced by hydrated cations, e.g. Na^+, Mg^{2+}, Ca^{2+}, etc., which are located in the interlamellar space. Such interlamellar cations are typically exchangeable, while the quantity of exchangeable cations shows the cation-exchange capacity (CEC) of the clay minerals. The Montmorillonites are aluminosilicate minerals which possess 2:1 layer phyllosilicates: two Si tetrahedral sheets are separated by one Al octahedral sheet (T-O-T) (Fig. 13.5). The isomorphic exchanges in the sheets, mostly in octahedral ones for Montmorillonite clays, create deficits of positive electric charges (Volzone et al. 2002). A fundamental

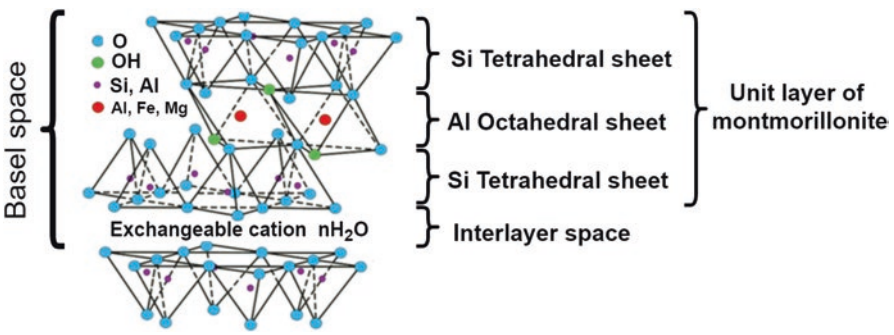

Fig. 13.5 Structure of Montmorillonite

characteristic of Montmorillonite is to absorb water and expand. Therefore, the volume of Montmorillonite increases, and the swelling pressure occurs (Fig. 13.6). The swelling behaviour of Montmorillonite is produced due to two mechanisms defined as crystalline swelling and osmotic swelling. These mechanisms work differently depending on the degree of hydration and the nature of cation in the interlayers.

In recent years, aluminosilicates, especially Montmorillonite, have been widely used as supports of TiO_2 for photocatalytic water treatment. Insertion of TiO_2 into aluminosilicates not only enhances the elimination of organic/inorganic pollutants via simple adsorption due to their high adsorption capabilities but also enhances the overall photocatalytic efficiency by increasing the concentration of species to be oxidized or reduced by active TiO_2 sites. Furthermore, the introduction of TiO_2 particles into the interlays of mineral clay leads to the formation of well-distributed TiO_2 nanoparticles with small size which increases the photocatalytic efficiency (Fig. 13.7). In addition, clay-based photocatalysts are easy to separate from the solution after the photocatalytic treatment. In general, an effective TiO_2 support (i) must be chemically

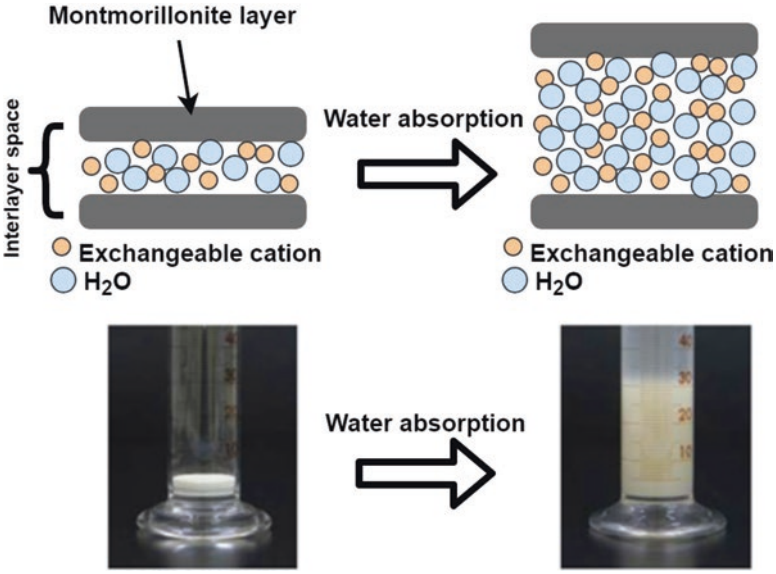

Fig. 13.6 Swelling of Montmorillonite

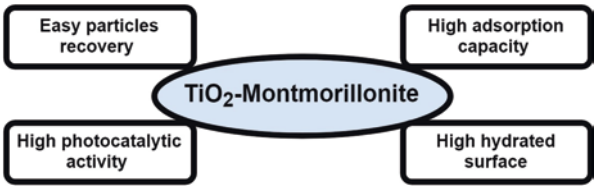

Fig. 13.7 Main advantages of TiO_2–Montmorillonite-based composites compared to TiO_2

inert, (ii) can form bonds with titanium dioxide without diminishing its photoactivity, (iii) has a large surface area and (iv) must be easy to remove after treatment.

13.3.1 Synthesis Methods

For the synthesis of TiO_2-clay/adsorbent-based photocatalysts, there are two ways (Fig. 13.8): (i) insertion/diffusion of TiO_2 nanoparticles powder (commercial or presynthesized) into material interlayers by diffusion and (ii) in situ synthesis of TiO_2 deposited into either material interlayers or on the external surface. For the in situ synthesis, the most applied, there are many techniques such as sol-gel, impregnation, chemical vapour deposition and hydrothermal. Various TiO_2–Montmorillonite have been synthesized using different methods for the photocatalytic removal of organics and heavy metals, and a brief comparison is shown in Table 13.1.

13.3.1.1 Sol-gel Method

Sol-gel has been widely used to design of TiO_2/porous support composites. In general, it involves hydrolysis polymerization, followed by drying and thermal treatment steps. The pillaring ways for the synthesis of pillared TiO_2/porous support are usually included in three steps: (i) Ti(VI)-containing compound is hydrolyzed to get $Ti(OH)_4$ sol particles; (ii) intercalation of $Ti(OH)_4$ sol particles into the Montmorillonite interlayers; and (iii) the mixture then is dried and calcined to transform the metal polyoxocations into TiO_2 pillars. However, most of $Ti(OH)_4$ colloidal could not introduce into the interlayer space of Montmorillonite and remained on the external surface, in which TiO_2–Montmorillonite sandwiched structure cannot be obtained. To solve this problem, many research groups have used organic surfactants in order to homogeneously intercalate TiO_2 nanoparticles within the interlayer space of Montmorillonite (Fig. 13.9). These surfactants usually facilitate

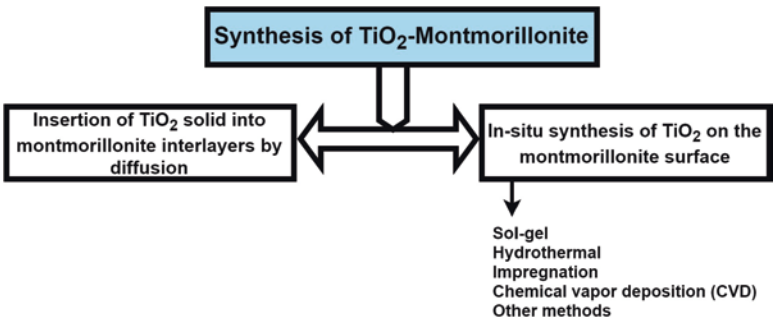

Fig. 13.8 Commonly used techniques for the synthesis of TiO_2–Montmorillonite composites

Table 13.1 TiO_2–Montmorillonite-based composites for the photocatalytic water remediation

Photocatalyst	Synthesis method	Light	Pollutant	References
TiO_2–M	Hydrothermal method with pH switching	UV	Methyl orange	Huo et al. (2018)
TiO_2–M	Solid diffusion	UV	Methylene blue	Liang et al. (2017)
TiO_2–M	Sol-gel	UV	1,4-Dioxane	Kameshima et al. (2009a)
TiO_2–M	Sol-gel	UV	As(V), As(III)	Li et al. (2012)
TiO_2–M	Sol-gel	UV	Hg(II)	Dou et al. (2011a, b)
TiO_2–M	Sol-gel	UV	Methylene blue	Chen et al. (2012)
TiO_2–M	Sol-gel using conventional heating and microwave heating	UV	Solophenyl red 3BL	Damardji et al. (2009a, b)
TiO_2–M	Sol-gel	UV	Di-n-butyl phthalate	Ooka et al. (2003)
			Diethyl phthalate	
			Dimethyl phthalate	
			Bisphenol-A	
M_1–TiO_2–M (M_1: Ag, au, Pd)	Sol-gel	UV, Vis	Chlorobenzene benzaldehyde	Mishra et al. (2018)
TiO_2–M	Sol-gel	UV	Congo red	Dvininov et al. (2009)
TiO_2–M	Sol-gel	UV	Methylene blue	Chen et al. (2014)
TiO_2–M	Electrophoretic deposition	UV	Methylene blue	Rastgar et al. (2013)
TiO_2–M	Intra-gallery templating	UV	Methylene blue	Yang et al. (2013)
TiO_2–M	Sol-gel	UV	Dimethachlor	Belessi et al. (2007)
TiO_2–M	Hydrothermal	UV	Methyl orange rhodamine B	Butman et al. (2018)
TiO_2–M	Impregnation	UV	Methylene blue remazol black	Sahel et al. (2014)
Ag–TiO_2–M				
TiO_2–M	Impregnation	UV	Chlorobenzene methylene blue	Mishra et al. (2017a, b)
TiO_2–M	Impregnation	UV	Methylene blue	Miao et al. (2006)
TiO_2–M	Solvothermal	UV	Methylene blue	Liu et al. (2009)
TiO_2–M	Hydrothermal method/ solid diffusion	UV	Methyl orange	Yuan et al. (2011)
TiO_2–M	Hydrothermal method/ solid diffusion	UV	2,4-Dichlorophenol	Zhang et al. (2015)
TiO_2–M	Sol-gel	UV	2,4-Dichlorophenol	Manova et al. (2010)
TiO_2–M	Sol-gel	UV	Methylene blue, *E. coli*	Fatimah (2012)
TiO_2–M	Hydrothermal method	UV	Pharmaceuticals	Hassani et al. (2017a, b)

(continued)

Table 13.1 (continued)

Photocatalyst	Synthesis method	Light	Pollutant	References
TiO_2–M	Impregnation	UV Solar	Crystal violet, rhodamine B, congo red, methylene blue methyl orange, Cr(VI)	Djellabi et al. (2014), Djellabi et al. (2016a), Djellabi et al. (2016b, c)
TiO_2–M	Impregnation	UV	Methylene blue	Rossetto et al. (2010)
TiO_2–M	Wet grinding in an agate mill	UV-Vis	Phenol	Ménesi et al. (2008)
TiO_2–M	Hydrothermal	UV	Trichloroethylene	Ooka et al. (1999)
Ag–TiO_2–M	Thermal decomposition method	UV	*S. aureus*, *E. coli*	Krishnan and Mahalingam (2017)
Ag–TiO_2–M	Microwave heating/ impregnation	UV, Vis	Chlorobenzene	Mishra et al. (2017a, b)
TiO_2–Fe–M	Impregnation	UV	Toluene	Liang et al. (2016)
TiO_2–Fe_3O_4–M	Sol-gel/coprecipitation under N_2	UV	Methylene blue	Chen et al. (2015)
CdS–M	Hydrothermal method	UV-Vis	Methylene blue rhodamine 6G	Boukhatem et al. (2013)
Fe(III)/ TiO_2–M	TiO_2 pillarization followed by Fe(III) ion exchange	UV	Methylene blue	Fatimah et al. (2015)
N–TiO_2–M	N-doped TiO_2 impregnation with Montmorillonite	Visible	Bisphenol-A	Hsing et al. (2018)
g-C_3N_4/ TiO_2–M	Hydrolysis, dehydroxylation and crystallization	Visible	Organics	CN105107542A
V–TiO_2–M	Sol-gel	UV-Vis	Sulforhodamine B	Chen et al. (2010), Chen et al. (2011)
C–TiO_2–M				
CdS/TiO_2–M	Hydrothermal synthesis	Visible	Methylene blue	Wang et al. (2015)
MgO–TiO_2–Al_2O_3/M	Inflating, intercalation and reassembling method	/	/	Dou et al. (2011a, b)
TiO_2–CeO_2–M	Water-based method	Solar	Parathion methyl	Henych et al. (2017)
SiO_2–TiO_2–M	Hydrothermal method/ solid diffusion	/	/	Kameshima et al. (2009b)
TiO_2–M/ PTP–SDS	In situ chemical oxidative polymerization	UV	Rhodamine 6G	Khalfaoui-Boutoumi et al. (2013)

the access of $Ti(OH)_4$ into the interlayer space of Montmorillonite. Therefore, this method not only improves the dispersion of TiO_2 onto Montmorillonite surface but also leads to improvement the pore size and the surface area by increase of basal space of the Montmorillonite.

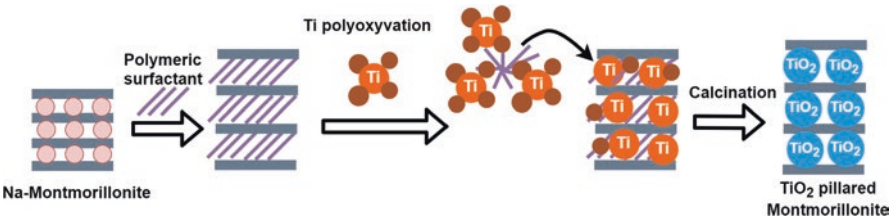

Fig. 13.9 Synthesis of TiO_2–Montmorillonite by sol-gel using organic surfactants

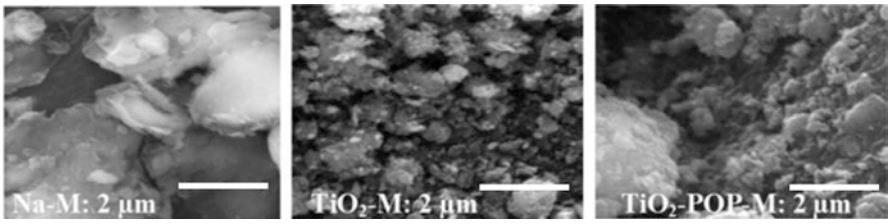

Fig. 13.10 SEM images of Na-Montmorillonite and TiO_2–Montmorillonite synthesized by sol-gel method. (Reproduced with permission: Chen et al. 2012)

Sun et al. (2015) have used cetyltrimethylammonium (CTA^+) surfactant to synthesis TiO_2–Montmorillonite by sol-gel method. They found that the basal space was enlarged from 15.54 Å for the original Ca-Montmorillonite sample to 38.71 Å for CTA^+-Montmorillonite. Tahir et al. (Tahir and Amin 2013) have synthesized TiO_2–Montmorillonite by sol-gel method using isopropanol as a surfactant. They reported that the Montmorillonite controls the crystal growth of TiO_2: the size of TiO_2 nanoparticles decreased from 18.73 (pure TiO_2) to 13.87 nm after adding the Montmorillonite, while the BET surface area and pore volume increased. Chen et al. (2012) have synthesized TiO_2–Montmorillonite by sol-gel method with the high-molecular-weight polymer surfactant POP (polyoxypropylene-backboned di-quaternary salt) as an expand species. They reported that the use of polymer surfactant POP leads to the formation of the delaminated structure and considerably improves the porosity and surface area of the composites. Also, the resulting TiO_2–Montmorillonite exhibited a good thermal stability after calcination at 800 °C. The anatase to rutile phase transformation was not detected even under calcination at 900 °C (SEM images in Fig. 13.10). On the other hand, they reported that the increase of POP amount leads to decrease the size of TiO_2 particles in the composite.

13.3.1.2 Hydrothermal Method

TiO_2–Montmorillonite composites can be also synthesized by hydrothermal method. It is carried out usually under controlled temperature or pressure using steel pressure vessels (autoclaves) with or without Teflon liners. The temperature is frequently elevated above the boiling point of water. Aydin Hassani et al. (2017a, b) have

synthesized TiO_2–Montmorillonite using cetyltrimethylammonium bromide (CTAB) as a surfactant, by hydrothermal method (Fig. 13.11). They found that the average crystalline size was 25 nm for pure TiO_2 and 20 nm for TiO_2 in TiO_2–Montmorillonite (SEM images are shown in Fig. 13.12). They suggested that the Montmorillonite can control the crystal growth in TiO_2. However, they obtained that the deposition of TiO_2 did not improve the basal space of the Montmorillonite, which could be explained by the deposition of TiO_2 nanoparticles on the external surface of the Montmorillonite. Zhou et al. (2014) have synthesized CdS–TiO_2–Montmorillonite by hydrothermal method. They reported that the small angle in the XRD spectrum was disappeared after the insertion of CdS–TiO_2 nanoparticles which indicates that the basal space of the Montmorillonite had been blocked by CdS–TiO_2 particles.

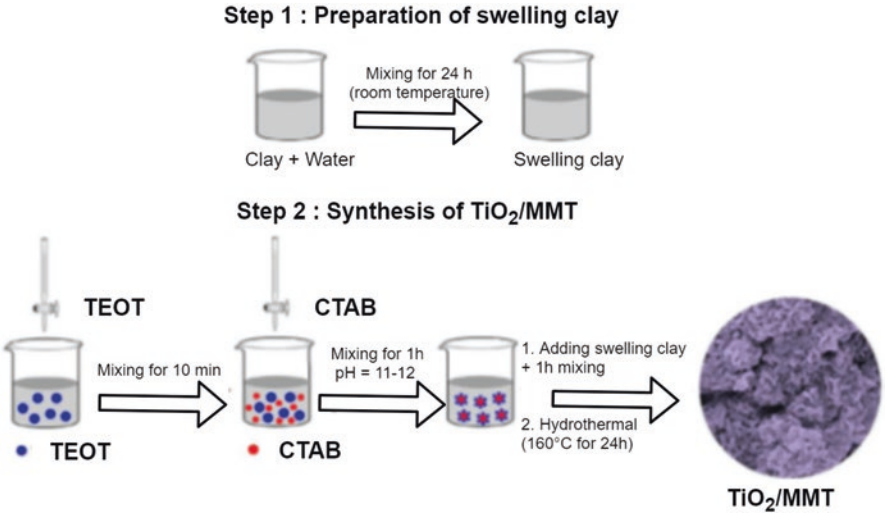

Fig. 13.11 Synthesis of TiO_2–Montmorillonite by hydrothermal method. (Reproduced with permission: Hassani et al. 2017a, b)

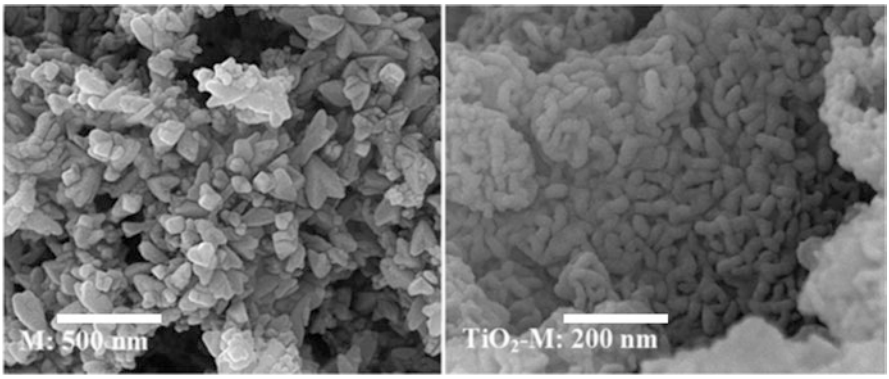

Fig. 13.12 SEM images of Na–Montmorillonite and TiO_2–Montmorrilonite synthesized by hydrothermal method. (Reproduced with permission: Hassani et al. 2017a, b)

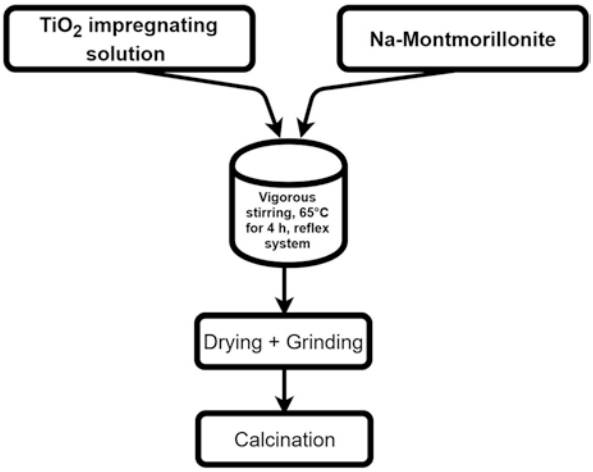

Fig. 13.13 Synthesis of TiO_2–Montmorillonite by impregnation method

13.3.1.3 Impregnation Method

The synthesis of TiO_2–Montmorillonite by impregnation could be simplified as is illustrated in Fig. 13.13, which includes three main steps: (i) contacting the Montmorillonite with the TiO_2 precursor solution, (ii) filtration and drying the composite and (3) calcination of the composite to form TiO_2 crystals.

Djellabi et al. (2016a, b, c) have synthesized TiO_2–Montmorillonite with different weight ratios (g/g) (5, 10, 20 and 30%) by impregnation with $TiCl_4$ (dissolved in C_2H_2) followed by calcination at 350 °C. They reported that the basal spacing of Montmorillonite decreases slightly with TiO_2 loading, while the surface area of all samples was similar to that of Na-Montmorillonite. On the other hand, the average crystallite size of anatase was estimated to be 14–20 nm for all samples (SEM images are shown in Fig. 13.14). Compared to sol-gel method, impregnation method usually does not improve the based space and the surface area since the deposition of TiO_2 nanoparticles takes place mostly on the external surface of the Montmorillonite, while the sandwiched structure could be obtained by sol-gel. Rossetto et al. (2010) have synthesized TiO_2–Montmorillonite samples using different kinds of Montmorillonite by impregnation with $TiCl_4$ (dissolved in cyclohexane), and they found that the surface area of some samples decreased after impregnation of TiO_2.

13.3.1.4 Solid Diffusion

Solid diffusion or power sintering is a simple method to make strong binding force between TiO_2 nanoparticles and porous supports thermal diffusion effect (Wang et al. 2018). Zhang et al. (2015) and Yuan et al. (2011) have synthesized TiO_2–Montmorillonite via the immobilization of pre-dispersed nanoscaled TiO_2 particles

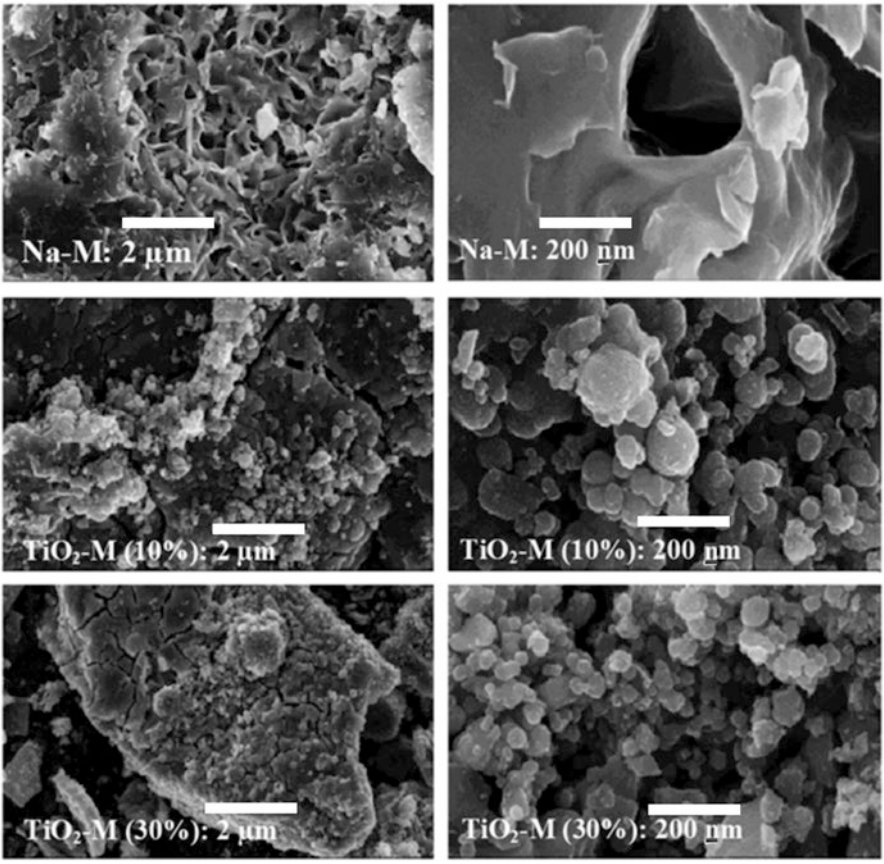

Fig. 13.14 SEM images of Na-Montmorillonite and TiO_2–Montmorillonite synthesized by impregnation method. (Reproduced with permission: Djellabi et al. 2016a, b, c)

onto external surface of Montmorillonite. Firstly, they prepared nanoscaled TiO_2 hydrothermal method with an average size less than 5 nm. Then, they mixed nanoscaled TiO_2-cetyltrimethylammonium bromide (CTAB) solution with swelling-Montmorillonite, and finally, the products were calcined at 500 °C. Yuan et al. (2011) reported that the nanoscaled TiO_2 (with 4.66 nm) could be intercalated into the interlayer of Montmorillonite due to the presence of CTAB (basal spacing increased from 1.26 to 1.87 nm and surface area increased from 28 to 67 m^2/g). Zhang et al. (2015) reported that the increase of CTAB surfactant increases slightly the basal spacing, while, the anatase-to-rutile transformation was observed during calcination at 500 °C. However, it was found that the characteristic reflection for the anatase phase at $2\theta = 25.3°$ was slightly decreased with CTAB increasing (from 0.1 to 0.5 wt.%). They explained that the high CTAB concentrations lead to decreasing numbers and increasing particle size deposited TiO_2 particles into the interlayer. With low CTAB amounts, more TiO_2 pillars can be immobilized in the interlayer

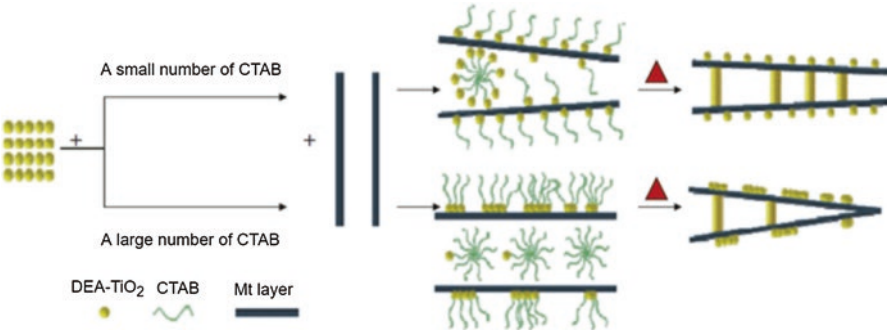

Fig. 13.15 Formation process of TiO_2-CTAB-Montmorillonite according to different CTAB contents. (Reproduced with permission: Zhang et al. 2015)

space, and at the same time, a number of TiO_2 particles with smaller size could be fixed on the external surface of Montmorillonite. On the contrary, with high CTAB concentrations, more CTAB species can block the pores of Montmorillonite, which inhibits the access of TiO_2 colloids to settle into the pores of Montmorillonite (as shown in Fig. 13.15).

Liang et al. (2017) have immobilized pure TiO_2 (P25, Degussa) onto external surface of Montmorillonite using power sintering method proceeding with the following steps: (i) Montmorillonite material and 1 g of P25-TiO_2 were mixed; (ii) a volume of ethanol was added, and the mixture was milled for 30 min and dried at 300 °C for 6 h; and (iii) the obtained solid was grinded. They prepared a series of TiO_2–Montmorillonite of different loads (40%T/M (TiO_2/Montmorillonite), 70%T/M, 80%T/M, 90%T/M, 95%T/M, 98%T/M). The results of TEM morphologies showed that the nano-TiO_2 is loaded successfully onto the Montmorillonite surface. However, when TiO_2 content increases, TiO_2 particles on Montmorillonite surface are prone to agglomeration (Fig. 13.16).

13.3.2 Mechanisms of Photocatalytic Removal of Contaminants by TiO_2–Montmorillonite

The immobilization of nanoscale TiO_2 particles onto the Montmorillonite can assist in improving the contact between the TiO_2 particles and pollutants via the so-called Adsorb & Shuttle *(A&S)* due to its adsorption capability and hydrophobicity property. In general, this concept is based on the use of highly adsorbing domains to increase the amount (concentration) of contaminants near TiO_2 photocatalytic sites and therefore enhance the overall efficiency of the photocatalytic process as shown schematically in Fig. 13.17. Nevertheless, a second mechanism by which the photocatalytic degradation of organic pollutants is obtained through the use of adsorbent support is the diffusion of hydroxyl radicals from TiO_2 from the photocatalytic sites to the adsorbed pollutants on the adsorptive domains, named as "Remote Degradation" (Fig. 13.17).

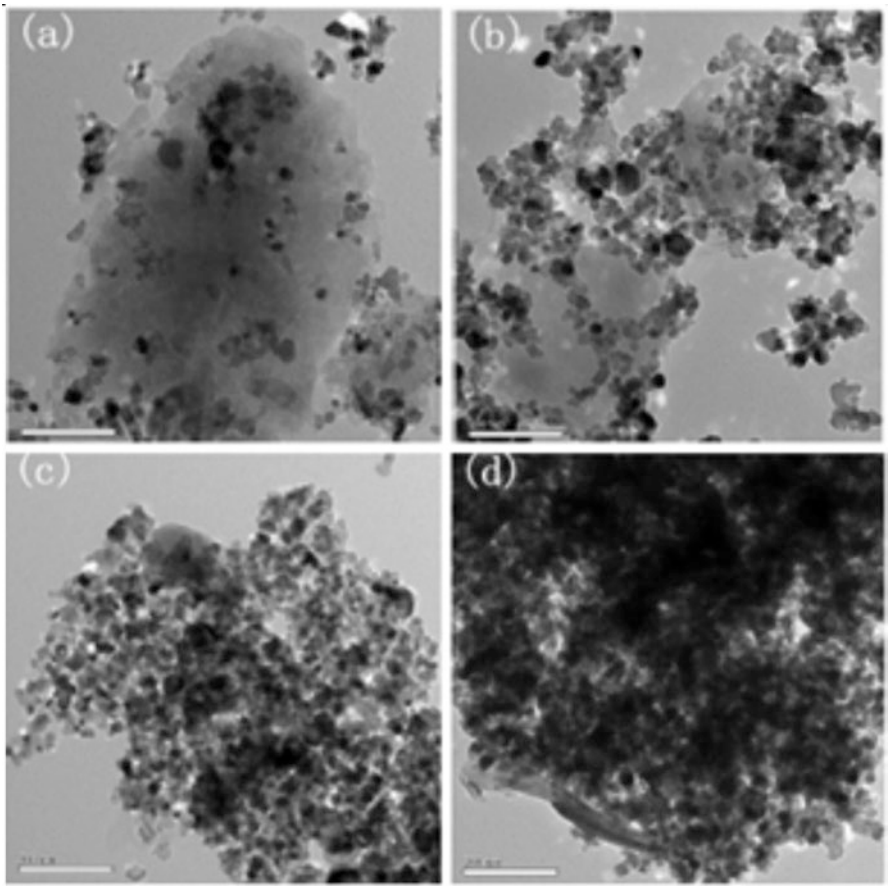

Fig. 13.16 TEM images of TiO_2–Montmorillonite synthesized by solid diffusion process with different load ratios (**a**) 70%T/M, (**b**) 80%T/M, (**c**) 90%T/M, and (**d**) 95%T/M. (Reproduced with permission: Liang et al. 2017)

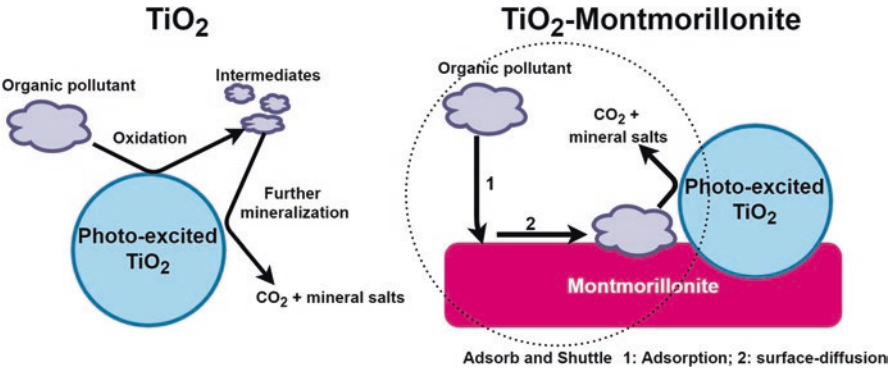

Fig. 13.17 Mechanisms of the photocatalytic removal of pollutants on the surface of TiO_2 and TiO_2–Montmorillonite

Many research studies reported that TiO_2–Montmorillonite composite was more efficient than commercial or synthesized naked TiO_2 (Rossetto et al. 2010; Dou et al. 2011a; Yuan et al. 2011; Chen et al. 2012; Liang et al. 2017; Mishra et al. 2017a, b; Butman et al. 2018). TiO_2–Montmorillonite can combine the adsorption and photocatalytic reaction to efficiently remove contaminants from water (Dvininov et al. 2009; Djellabi et al. 2014). Moreover, TiO_2–Montmorillonite-based composites may retain reaction by-products that are produced during the photocatalytic reaction for further mineralization. Additionally, employing of TiO_2–Montmorillonite overcomes the issue of photocatalyst separation in water purification systems. Because the TiO_2 loading onto Montmorillonite can affect the morphology, surface area, pore size and TiO_2 particle size, it has an important impact on the *Adsorb & Shuttle process*. For higher A&S efficiency, the optimum diffusion distance (distance between the adsorbing domains and TiO_2 sites) should be obtained. Nevertheless, the optimal TiO_2 loading value depends not only on the type of TiO_2–Montmorillonite characteristics but also on the type of pollutant. Higher interaction between the pollutant species and TiO_2–Montmorillonite surface is likely to push the optimum TiO_2 loading towards small values, since high TiO_2 content on Montmorillonite may require a large diffusion distance of pollutant molecules that adsorb strongly on the surface. For the pollutant molecules that adsorb hardly on the surface of TiO_2–Montmorillonite, the reverse is true. It is worth to note that, there is a bottleneck state, in which, the excessive TiO_2 content can block the penetration of light irradiation. At the optimal TiO_2 loading value, the TiO_2–Montmorillonite needs to adsorb contaminants efficiently and then oxidizes/mineralizes them photocatalytically to regenerate the surface for recycling. Djellabi et al. (2016a) have studied the effect of TiO_2 loading onto the Montmorillonite for the photocatalytic removal of Cr(VI) and crystal violet under sunlight. They have synthesized TiO_2–Montmorillonite with different weight ratios (g/g) (5, 10, 20 and 30%), and they reported that the dark adsorption of crystal violet decreases with TiO_2 content increasing, while the Cr(VI) species adsorbs very hardly on TiO_2–Montmorillonite surface (~ 12% for all samples). For the photocatalytic removal under sunlight, they reported that the sample with 10% of TiO_2 loading was the most efficient for crystal violet photodegradation, while for Cr(VI) reduction, the removal rate increases proportionally with TiO_2 loading, and the sample 30% was the most efficient. In a straightforward manner, the fact that the efficiency of TiO_2–Montmorillonite varies from one pollutant to another, using the same sample with 10% of TiO_2 loading, Djellabi et al. (2014) reported that the efficiency of TiO_2–Montmorillonite for the removal of five dyes under UV light was more pronounced for cationic dyes than anionic in the order crystal violet (97.1%) > methylene blue (93.20%) > rhodamine B (79.8%) > methyl orange (36.1%) > congo red (22.6%), which is due to the strong interaction between cationic dyes and the negatively charged TiO_2–Montmorillonite surface.

Dou et al. (2011a) reported that TiO_2–Montmorillonite (with a 22 wt% TiO_2 load) had higher adsorption and photocatalytic activities than synthesized TiO_2 nanoparticles for the removal of Hg(II) from water. They observed that both photocatalysts turned black with Hg(0) nanoparticles under UV illumination. They found

that the photo-efficiency of TiO_2–Montmorillonite and TiO_2 nanoparticles decreases after 40 min due to the deposition of Hg metal on the TiO_2 surface, resulting in less reactivity. Li et al. (2012) have used TiO_2–Montmorillonite as an adsorbent to remove As(III) and As(V) from water with or without UV irradiation. They reported that, with UV irradiation of TiO_2–Montmorillonite, the removal rate of As(III) and As(V) increased from 94.58% to 97.71% and from 98.56% to 99.65%, respectively. They suggested that As(III) oxidation to As(V) takes place by TiO_2 particles, followed by fast As(V) adsorption on TiO_2–Montmorillonite surface.

The pore size of TiO_2–Montmorillonite can also affect the A&S process. As explained before, the synthesis conditions including the method, type of surfactants, calcination and TiO_2 loading could affect directly the pore size of TiO_2–Montmorillonite. In general, based on the pore size, materials could be divided into three groups: microporous (< 2 nm), mesoporous (2–50 nm) and macroporous (> 50 nm). Meso- and macroporous adsorbents are suitable for the adsorption/absorption of contaminant molecules with different sizes, which in turn facilitate their photocatalytic decomposition. This was indeed observed by Yuan et al. (2011), who reported that the TiO_2–Montmorillonite sample with higher pore size and pore volume exhibited a higher photocatalytic efficiency for organic molecules. Chen et al. (2012) reported that the photoactivity of TiO_2–Montmorillonite was not a function of TiO_2 loading of the composite photocatalyst, but it depends on the contact between TiO_2–Montmorillonite surface and the dye species. Yang et al. (2013) have synthesized TiO_2–Montmorillonite samples with ordered interlayer mesoporous structure, and they reported that the photocatalytic efficiency for the degradation of methylene blue increases proportionally with increase of pore size.

Butman et al. (2018) have synthesized TiO_2–Montmorillonite samples with high degree of crystallinity (nanocrystals) for degradation of methyl orange and rhodamine B under UV. They reported that the high decolourization rate was due to the higher degree of crystallinity for TiO_2 pillars and higher porosity. On the other hand, they suggested that the anatase and rutile phase ratio can strongly influence the rate of photocatalytic oxidation of dyes. Also, they proposed that the formation of Ti–O–Si cross-links between pillars and silicate layers of Montmorillonite may limit the electron/hole recombination. Therefore, the higher the crystallites of TiO_2, the greater the number of cross-linking bonds can be formed; thus, a higher photocatalytic efficiency is found.

Mishra et al. (2018) have prepared metal-loaded TiO_2–Montmorillonite composites (M = Ag, Au, Pd; 1% by wt.) for the photodegradation of chlorobenzene and benzaldehyde under UV and visible light. It was found that the surface area and pore size increased slightly in the presence of metals. They reported that both the dark adsorption and the photocatalytic degradation of chlorobenzene and benzaldehyde by Metal–TiO_2–Montmorillonite were higher than TiO_2–Montmorillonite under UV and visible irradiations. It is worth to note that, based on their results, TiO_2–Montmorillonite exhibited a photocatalytic activity under visible light. They found that, among the as-synthesized composites, Ag–TiO_2–Montmorillonite shows the highest photocatalytic efficiency for chlorobenzene and benzaldehyde degrada-

tion under visible light. They suggested that the high photocatalytic performance of Ag–TiO_2–Montmorillonite may be due to the high excitation lifetime (2.60 ns).

13.4 Conclusions

- Coupling of nanoscale TiO_2 particles with Montmorillonite promotes the photocatalytic performance for the removal of organic pollutants and heavy metals.
- Montmorillonite samples with high specific surfaces areas, high adsorption capacity and high hydrophobicity could be a good choice for the synthesis of effective TiO_2–Montmorillonite.
- Many researchers reported that the Montmorillonite can control the crystal growth and the thermal stability of TiO_2 better than naked TiO_2.
- The use of polymer surfactants during the synthesis of TiO_2–Montmorillonite such as cetyltrimethylammonium (CTA^+) and polyoxypropylene-backboned diquaternary (POP) allows intercalating homogeneously TiO_2 nanoparticles within the interlayer space of Montmorillonite (obtain a sandwich structure) and reduces the agglomeration of TiO_2 particles, and it improves the pore size and the surface area by increasing of basal space of the Montmorillonite. It is worth noting that the concentration of surfactant should be optimized.
- TiO_2 loading in the Montmorillonite can affect significantly the structure of TiO_2–Montmorillonite depending on the synthesis conditions; at high loading, TiO_2 is prone to agglomerate and block the pore of the Montmorillonite.
- The photocatalytic removal of organic pollutants and heavy metals is carried out through the so-called Adsorb & Shuttle (A&S), in which pollutants adsorbed on the adsorbing domains (Montmorillonite) diffuse on the surface to the TiO_2 photocatalytic. The Adsorb & Shuttle process efficiency depends strongly on the TiO_2–Montmorillonite characteristics (TiO_2 loading, pore size, adsorption capacity and TiO_2 particle size) as well as the type of pollutant.
- Unlike naked nanoparticles TiO_2, TiO_2–Montmorillonite is a low-cost and environmentally friendly photocatalyst which prevents the release of TiO_2 nanoparticles to the environment, and it can retain reaction by-products that are produced during the photocatalytic reaction for further mineralization.

References

Anggraini DI, Hp ES, Santosa EOG (2016) Photocatalytic reduction of Cu(II) ion and TiO_2-catalyzed paracetamol photodegradation as an alternative method in waste treatment. ALCHEMY Jurnal Penelitian Kimia 11(2):163–174. https://doi.org/10.20961/alchemy.11.2.726.163-174

Belessi V, Lambropoulou D, Konstantinou I, Katsoulidis A, Pomonis P, Petridis D, Albanis T (2007) Structure and photocatalytic performance of TiO_2/clay nanocomposites for the degradation of dimethachlor. Appl Catal B Environ 73(3–4):292–299. https://doi.org/10.1016/j.apcatb.2006.12.011

Belver C, Bedia J, Rodriguez J (2015) Titania–clay heterostructures with solar photocatalytic applications. Appl Catal B Environ 176:278–287. https://doi.org/10.1016/j.apcatb.2015.04.004

Belver C, Bedia J, Álvarez-Montero M, Rodriguez J (2016) Solar photocatalytic purification of water with Ce-doped TiO_2/clay heterostructures. Catal Today 266:36–45. https://doi.org/10.1016/j.cattod.2015.09.025

Belver C, Han C, Rodriguez J, Dionysiou D (2017) Innovative W-doped titanium dioxide anchored on clay for photocatalytic removal of atrazine. Catal Today 280:21–28. https://doi.org/10.1016/j.cattod.2016.04.029

Bhattacharyya A, Kawi S, Ray M (2004) Photocatalytic degradation of orange II by TiO_2 catalysts supported on adsorbents. Catal Today 98(3):431–439. https://doi.org/10.1016/j.cattod.2004.08.010

Boukhatem H, Djouadi L, Abdelaziz N, Khalaf H (2013) Synthesis, characterization and photocatalytic activity of CdS–montmorillonite nanocomposites. Appl Clay Sci 72:44–48. https://doi.org/10.1016/j.clay.2013.01.011

Butman MF, Ovchinnikov NL, Karasev NS, Kochkina NE, Agafonov AV, Vinogradov AV (2018) Photocatalytic and adsorption properties of TiO2-pillared montmorillonite obtained by hydrothermally activated intercalation of titanium polyhydroxo complexes. Beilstein J Nanotechnol 9:364. https://doi.org/10.3762/bjnano.9.36

Byrne JA, Eggins BR (1998) Photoelectrochemistry of oxalate on particulate TiO_2 electrodes. J Electroanal Chem 457(1–2):61–72. https://doi.org/10.1016/S0022-0728(98)00304-0

Byrne C, Subramanian G, Pillai SC (2017) Recent advances in photocatalysis for environmental applications. J Environ Chem Eng. https://doi.org/10.1016/j.jece.2017.07.080

Chen K, Li J, Li J, Zhang Y, Wang W (2010) Synthesis and characterization of TiO2–montmorillonites doped with vanadium and/or carbon and their application for the photodegradation of sulforhodamine B under UV–vis irradiation. Colloids Surf A Physicochem Eng Asp 360(1–3):47–56. https://doi.org/10.1016/j.colsurfa.2010.02.005

Chen K, Li J, Wang W, Zhang Y, Wang X, Su H (2011) The preparation of vanadium-doped TiO2–montmorillonite nanocomposites and the photodegradation of sulforhodamine B under visible light irradiation. Appl Surf Sci 257(16):7276–7285. https://doi.org/10.1016/j.apsusc.2011.03.104

Chen D, Zhu Q, Zhou F, Deng X, Li F (2012) Synthesis and photocatalytic performances of the TiO2 pillared montmorillonite. J Hazard Mater 235:186–193. https://doi.org/10.1016/j.jhazmat.2012.07.038

Chen D, Zhu H, Wang X (2014) A facile method to synthesize the photocatalytic TiO_2/montmorillonite nanocomposites with enhanced photoactivity. Appl Surf Sci 319:158–166. https://doi.org/10.1016/j.apsusc.2014.05.085

Chen W, Xiao H, Xu H, Ding T, Gu Y (2015) Photodegradation of methylene blue by TiO2-Fe3O4-bentonite magnetic Nanocomposite. Int J Photoenergy 2015:1. https://doi.org/10.1155/2015/591428

Cristante VM, Araujo AB, Jorge S, Florentino AO, Valente JP, Padilha PM (2006) Enhanced photocatalytic reduction of Hg (II) in aqueous medium by 2-aminothiazole-modified TiO2 particles. J Braz Chem Soc 17(3):453–457. https://doi.org/10.1590/S0103-50532006000300004

Damardji B, Khalaf H, Duclaux L, David B (2009a) Preparation of TiO2-pillared montmorillonite as photocatalyst Part I. Microwave calcination, characterisation, and adsorption of a textile azo dye. Appl Clay Sci 44(3–4):201–205. https://doi.org/10.1016/j.clay.2008.12.010

Damardji B, Khalaf H, Duclaux L, David B (2009b) Preparation of TiO2-pillared montmorillonite as photocatalyst Part II: photocatalytic degradation of a textile azo dye. Appl Clay Sci 45(1–2):98–104. https://doi.org/10.1016/j.clay.2009.04.002

Djellabi R, Ghorab M (2015a) Photoreduction of toxic chromium using TiO2-immobilized under natural sunlight: effects of some hole scavengers and process parameters. Desalin Water Treat 55(7):1900–1907. https://doi.org/10.1080/19443994.2014.927335

Djellabi R, Ghorab M (2015b) Solar photocatalytic decolourization of crystal violet using supported TiO2: effect of some parameters and comparative efficiency. Desalin Water Treat 53(13):3649–3655. https://doi.org/10.1080/19443994.2013.873354

Djellabi R, Ghorab M, Cerrato G, Morandi S, Gatto S, Oldani V, Di Michele A, Bianchi C (2014) Photoactive TiO2–montmorillonite composite for degradation of organic dyes in water. J Photochem Photobiol A Chem 295:57–63. https://doi.org/10.1016/j.jphotochem.2014.08.017

Djellabi R, Fouzi Ghorab M, Bianchi C, Cerrato G, Morandi S (2016a) Removal of crystal violet and hexavalent chromium using TiO2-bentonite under sunlight: effect of TiO2 content. J Chem Eng Process Technol 7(01):1–8. https://doi.org/10.4172/2157-7048.1000276

Djellabi R, Ghorab FM, Nouacer S, Smara A, Khireddine O (2016b) Cr (VI) photocatalytic reduction under sunlight followed by Cr (III) extraction from TiO2 surface. Mater Lett 176:106–109. https://doi.org/10.1016/j.matlet.2016.04.090

Djellabi R, Ghorab MF, Bianchi CL, Cerrato G, Morandi S (2016c) Recovery of hexavalent chromium from water using photoactive TiO2-montmorillonite under sunlight. Mediterranean J Chem 5(3):442–449. https://doi.org/10.13171/mjc53/016041311/djellabi

Djellabi R, Ghorab MF, Sehili T (2017) Simultaneous removal of methylene blue and hexavalent chromium from water using TiO2/Fe (III)/H2O2/sunlight. CLEAN–Soil Air Water 45(6). https://doi.org/10.1002/clen.201500379

Dou B, Chen H, Song Y, Tan C (2011a) Synthesis and characterization of heterostructured nanohybrid of MgO–TiO2–Al2O3/montmorillonite. Mater Chem Phys 130(1–2):63–66. https://doi.org/10.1016/j.matchemphys.2011.05.035

Dou B, Dupont V, Pan W, Chen B (2011b) Removal of aqueous toxic Hg (II) by synthesized TiO2 nanoparticles and TiO2/montmorillonite. Chem Eng J 166(2):631–638. https://doi.org/10.1016/j.cej.2010.11.035

Du Y, Zheng P (2014) Adsorption and photodegradation of methylene blue on TiO 2-halloysite adsorbents. Korean J Chem Eng 31(11):2051–2056. https://doi.org/10.1007/s11814-014-0162-8

Dvininov E, Popovici E, Pode R, Cocheci L, Barvinschi P, Nica V (2009) Synthesis and characterization of TiO2-pillared Romanian clay and their application for azoic dyes photodegradation. J Hazard Mater 167(1–3):1050–1056. https://doi.org/10.1016/j.jhazmat.2009.01.105

Fagan R, McCormack DE, Dionysiou DD, Pillai SC (2016) A review of solar and visible light active TiO2 photocatalysis for treating bacteria, cyanotoxins and contaminants of emerging concern. Mater Sci Semicond Process 42:2–14. https://doi.org/10.1016/j.mssp.2015.07.052

Fatimah I (2012) Composite of TiO2-montmorillonite from Indonesia and its photocatalytic properties in methylene blue and E. Coli reduction. J Mater Environ Sci 3(5):983–992

Fatimah I, Sumarlan I, Alawiyah T (2015) Fe (III)/TiO2-montmorillonite photocatalyst in photo-Fenton-like degradation of methylene blue. Int J Chem Eng 2015:1. https://doi.org/10.1155/2015/485463

Fogler HS (2006) Elements of chemical reaction engineering, 4th edn. Prentice Hall, Upper Saddle River, pp 869–878

Fontana KB, Lenzi GG, Seára EC, Chaves ES (2018) Comparison of photocatalysis and photolysis processes for arsenic oxidation in water. Ecotoxicol Environ Saf 151:127–131. https://doi.org/10.1016/j.ecoenv.2018.01.001

Fujishima A, Rao TN, Tryk DA (2000) Titanium dioxide photocatalysis. J Photochem Photobiol C: Photochem Rev 1(1):1–21. https://doi.org/10.1016/S1389-5567(00)00002-2

Gebru KA, Das C (2017) Removal of Pb (II) and Cu (II) ions from wastewater using composite electrospun cellulose acetate/titanium oxide (TiO2) adsorbent. J Water Process Eng 16:1–13. https://doi.org/10.1016/j.jwpe.2016.11.008

Guo Y, Guo Y, Wang X, Li P, Kong L, Wang G, Li X, Liu Y (2017) Enhanced photocatalytic reduction activity of uranium (vi) from aqueous solution using the Fe 2 O 3–graphene oxide nanocomposite. Dalton Trans 46(43):14762–14770. https://doi.org/10.1039/C7DT02639K

Hashimoto K, Irie H, Fujishima A (2005) TiO2 photocatalysis: a historical overview and future prospects. Jpn J Appl Phys 44(12R):8269. https://doi.org/10.1143/JJAP.44.8269

Hassani A, Khataee A, Karaca S, Fathinia M (2017a) Degradation of mixture of three pharmaceuticals by photocatalytic ozonation in the presence of TiO2/montmorillonite nanocomposite: simultaneous determination and intermediates identification. J Environ Chem Eng 5(2):1964–1976. https://doi.org/10.1016/j.jece.2017.03.032

Hassani A, Khataee A, Karaca S, Karaca C, Gholami P (2017b) Sonocatalytic degradation of ciprofloxacin using synthesized TiO2 nanoparticles on montmorillonite. Ultrason Sonochem 35:251–262. https://doi.org/10.1016/j.ultsonch.2016.09.027

Henych J, Kormunda M, Šťastný M, Janoš P, Vomáčka P, Matoušek J, Štengl V (2017) Water-based synthesis of TiO2/CeO2 composites supported on plasma-treated montmorillonite for parathion methyl degradation. Appl Clay Sci 144:26–35. https://doi.org/10.1016/j.clay.2017.05.001

Herrmann J-M (1999) Heterogeneous photocatalysis: fundamentals and applications to the removal of various types of aqueous pollutants. Catal Today 53(1):115–129. https://doi.org/10.1016/S0920-5861(99)00107-8

Hsing J, Kameshima Y, Nishimoto S, Miyake M (2018) Preparation of carbon-modified N–TiO2/montmorillonite composite with high photocatalytic activity under visible light radiation. J Ceram Soc Jpn 126(4):230–235. https://doi.org/10.2109/jcersj2.17235

Huo M, Guo H, Jiang Y, Ju H, Xue B, Li F (2018) A facile method of preparing sandwich layered TiO2 in between montmorillonite sheets and its enhanced UV-light photocatalytic activity. J Photochem Photobiol A Chem 358:121–129. https://doi.org/10.1016/j.jphotochem.2018.02.012

Kabra K, Chaudhary R, Sawhney R (2008) Solar photocatalytic removal of cu (II), Ni (II), Zn (II) and Pb (II): speciation modeling of metal–citric acid complexes. J Hazard Mater 155(3):424–432. https://doi.org/10.1016/j.jhazmat.2007.11.083

Kajitvichyanukul P, Chenthamarakshan C, Rajeshwar K, Qasim S (2002) Photocatalytic reactivity of thallium (I) species in aqueous suspensions of titania. J Electroanal Chem 519(1–2):25–32. https://doi.org/10.1016/S0022-0728(01)00709-4

Kameshima Y, Tamura Y, Nakajima A, Okada K (2009a) Preparation and properties of TiO2/montmorillonite composites. Appl Clay Sci 45(1–2):20–23. https://doi.org/10.1016/j.clay.2009.03.005

Kameshima Y, Yoshizawa A, Nakajima A, Okada K (2009b) Solid acidities of SiO2–TiO2/montmorillonite composites synthesized under different pH conditions. Appl Clay Sci 46(2):181–184. https://doi.org/10.1016/j.clay.2009.08.001

Khalfaoui-Boutoumi N, Boutoumi H, Khalaf H, David B (2013) Synthesis and characterization of TiO2–Montmorillonite/Polythiophene-SDS nanocomposites: application in the sonophotocatalytic degradation of rhodamine 6G. Appl Clay Sci 80:56–62. https://doi.org/10.1016/j.clay.2013.06.005

Krishnan B, Mahalingam S (2017) Ag/TiO2/bentonite nanocomposite for biological applications: synthesis, characterization, antibacterial and cytotoxic investigations. Adv Powder Technol 28(9):2265–2280. https://doi.org/10.1016/j.apt.2017.06.007

Lee S-Y, Park S-J (2013) TiO2 photocatalyst for water treatment applications. J Ind Eng Chem 19(6):1761–1769. https://doi.org/10.1016/j.jiec.2013.07.012

Lee WH, Teh SJ, Chou PM, Lai CW (2017) Photocatalytic reduction of aqueous mercury (II) using hybrid WO3-TiO2 nanotubes film. Curr Nanosci 13(6):616–624. https://doi.org/10.2174/1573413713666170616084447

Lenzi G, Fávero C, Colpini L, Bernabe H, Baesso M, Specchia S, Santos O (2011) Photocatalytic reduction of Hg (II) on TiO2 and Ag/TiO2 prepared by the sol–gel and impregnation methods. Desalination 270(1–3):241–247. https://doi.org/10.1016/j.desal.2010.11.051

Li Y, Liu JR, Jia SY, Guo JW, Zhuo J, Na P (2012) TiO2 pillared montmorillonite as a photoactive adsorbent of arsenic under UV irradiation. Chem Eng J 191:66–74. https://doi.org/10.1016/j.cej.2012.02.058

Liang X, Qi F, Liu P, Wei G, Su X, Ma L, He H, Lin X, Xi Y, Zhu J (2016) Performance of Ti-pillared montmorillonite supported Fe catalysts for toluene oxidation: the effect of Fe on catalytic activity. Appl Clay Sci 132:96–104. https://doi.org/10.1016/j.clay.2016.05.022

Liang H, Wang Z, Liao L, Chen L, Li Z, Feng J (2017) High performance photocatalysts: Montmorillonite supported-nano TiO2 composites. Optik Int J Light Electron Opt 136:44–51. https://doi.org/10.1016/j.ijleo.2017.02.018

Litter MI (1999) Heterogeneous photocatalysis: transition metal ions in photocatalytic systems. Appl Catal B Environ 23(2–3):89–114. https://doi.org/10.1016/S0926-3373(99)00069-7

Litter MI (2009) Treatment of chromium, mercury, lead, uranium, and arsenic in water by heterogeneous photocatalysis. Adv Chem Eng 36:37–67. https://doi.org/10.1016/S0065-2377(09)00402-5

Litter MI (2015) Mechanisms of removal of heavy metals and arsenic from water by TiO2-heterogeneous photocatalysis. Pure Appl Chem 87(6):557–567. https://doi.org/10.1515/pac-2014-0710

Litter MI (2017) Last advances on TiO2-photocatalytic removal of chromium, uranium and arsenic. Curr Opin Green Sustain Chem 6:150–158. https://doi.org/10.1016/j.cogsc.2017.04.002

Liu J, Dong M, Zuo S, Yu Y (2009) Solvothermal preparation of TiO2/montmorillonite and photocatalytic activity. Appl Clay Sci 43(2):156–159. https://doi.org/10.1016/j.clay.2008.07.016

López-Muñoz M-J, Aguado J, van Grieken R, Marugán J (2009) Simultaneous photocatalytic reduction of silver and oxidation of cyanide from dicyanoargentate solutions. Appl Catal B Environ 86(1–2):53–62. https://doi.org/10.1016/j.apcatb.2008.07.022

López-Muñoz M-J, Arencibia A, Cerro L, Pascual R, Melgar Á (2016) Adsorption of hg (II) from aqueous solutions using TiO2 and titanate nanotube adsorbents. Appl Surf Sci 367:91–100. https://doi.org/10.1016/j.apsusc.2016.01.109

Lu M (2013) Photocatalysis and water purification: from fundamentals to recent applications. Wiley, Weinheim. ISBN:978-3-527-33187-1

Mahalakshmi M, Priya SV, Arabindoo B, Palanichamy M, Murugesan V (2009) Photocatalytic degradation of aqueous propoxur solution using TiO2 and Hβ zeolite-supported TiO2. J Hazard Mater 161(1):336–343. https://doi.org/10.1016/j.jhazmat.2008.03.098

Mahlamvana F, Kriek R (2014) Photocatalytic reduction of platinum (II and IV) from their chloro complexes in a titanium dioxide suspension in the absence of an organic sacrificial reducing agent. Appl Catal B Environ 148:387–393. https://doi.org/10.1016/j.apcatb.2013.11.011

Mahlamvana F, Kriek R (2015) Photocatalytic reduction of [RhCln (H2O) 6− n] 3− n (n= 0–6) in a titanium dioxide suspension: the role of structurally different sacrificial reducing agents. Appl Catal B Environ 162:445–453. https://doi.org/10.1016/j.apcatb.2014.06.042

Malato S, Fernández-Ibáñez P, Maldonado MI, Blanco J, Gernjak W (2009) Decontamination and disinfection of water by solar photocatalysis: recent overview and trends. Catal Today 147(1):1–59. https://doi.org/10.1016/j.cattod.2009.06.018

Manova E, Aranda P, Martín-Luengo MA, Letaïef S, Ruiz-Hitzky E (2010) New titania-clay nanostructured porous materials. Microporous Mesoporous Mater 131(1–3):252–260. https://doi.org/10.1016/j.micromeso.2009.12.031

Marinho BA, Djellabi R, Cristóvão RO, Loureiro JM, Boaventura RA, Dias MM, Lopes JCB, Vilar VJ (2017) Intensification of heterogeneous TiO2 photocatalysis using an innovative micro–meso-structured-reactor for Cr (VI) reduction under simulated solar light. Chem Eng J 318:76–88. https://doi.org/10.1016/j.cej.2016.05.077

Marinho BA, Cristóvão RO, Djellabi R, Caseiro A, Miranda SM, Loureiro JM, Boaventura RA, Dias MM, Lopes JCB, Vilar VJ (2018) Strategies to reduce mass and photons transfer limitations in heterogeneous photocatalytic processes: hexavalent chromium reduction studies. J Environ Manag 217:555–564. https://doi.org/10.1016/j.jenvman.2018.04.003

Ménesi J, Körösi L, Bazsó É, Zöllmer V, Richardt A, Dékány I (2008) Photocatalytic oxidation of organic pollutants on titania–clay composites. Chemosphere 70(3):538–542. https://doi.org/10.1016/j.chemosphere.2007.06.049

Miao S, Liu Z, Han B, Zhang J, Yu X, Du J, Sun Z (2006) Synthesis and characterization of TiO2–montmorillonite nanocomposites and their application for removal of methylene blue. J Mater Chem 16(6):579–584. https://doi.org/10.1039/B511426H

MiarAlipour S, Friedmann D, Scott J, Amal R (2018) TiO2/porous adsorbents: recent advances and novel applications. J Hazard Mater 341:404–423. https://doi.org/10.1016/j.jhazmat.2017.07.070

Mishra A, Mehta A, Sharma M, Basu S (2017a) Enhanced heterogeneous photodegradation of VOC and dye using microwave synthesized TiO2/clay nanocomposites: a comparison study of different type of clays. J Alloys Compd 694:574–580. https://doi.org/10.1016/j.jallcom.2016.10.036

Mishra A, Mehta A, Sharma M, Basu S (2017b) Impact of ag nanoparticles on photomineralization of chlorobenzene by TiO2/bentonite nanocomposite. J Environ Chem Eng 5(1):644–651. https://doi.org/10.1016/j.jece.2016.12.042

Mishra A, Mehta A, Kainth S, Basu S (2018) Effect of different plasmonic metals on photocatalytic degradation of volatile organic compounds (VOCs) by bentonite/M-TiO2 nanocomposites under UV/visible light. Appl Clay Sci 153:144–153. https://doi.org/10.1016/j.clay.2017.11.040

Mohamed R, Salam MA (2014) Photocatalytic reduction of aqueous mercury (II) using multi-walled carbon nanotubes/Pd-ZnO nanocomposite. Mater Res Bull 50:85–90. https://doi.org/10.1016/j.materresbull.2013.10.031

Murruni L, Conde F, Leyva G, Litter MI (2008) Photocatalytic reduction of Pb (II) over TiO2: new insights on the effect of different electron donors. Appl Catal B Environ 84(3–4):563–569. https://doi.org/10.1016/j.apcatb.2008.05.012

Nakata K, Fujishima A (2012) TiO2 photocatalysis: design and applications. J Photochem Photobiol C: Photochem Rev 13(3):169–189. https://doi.org/10.1016/j.jphotochemrev.2012.06.001

Ooka C, Akita S, Ohashi Y, Horiuchi T, Suzuki K, Komai S-i, Yoshida H, Hattori T (1999) Crystallization of hydrothermally treated TiO2 pillars in pillared montmorillonite for improvement of the photocatalytic activity. J Mater Chem 9(11):2943–2952. https://doi.org/10.1039/A901421G

Ooka C, Yoshida H, Horio M, Suzuki K, Hattori T (2003) Adsorptive and photocatalytic performance of TiO2 pillared montmorillonite in degradation of endocrine disruptors having different hydrophobicity. Appl Catal B Environ 41(3):313–321. https://doi.org/10.1016/S0926-3373(02)00169-8

Özcan AS, Erdem B, Özcan A (2005) Adsorption of acid blue 193 from aqueous solutions onto BTMA-bentonite. Colloids Surf A Physicochem Eng Asp 266(1–3):73–81. https://doi.org/10.1016/j.colsurfa.2005.06.001

Petronella F, Truppi A, Ingrosso C, Placido T, Striccoli M, Curri M, Agostiano A, Comparelli R (2017) Nanocomposite materials for photocatalytic degradation of pollutants. Catal Today 281:85–100. https://doi.org/10.1016/j.cattod.2016.05.048

Rastgar M, Zolfaghari A, Mortaheb H, Sayahi H, Naderi H (2013) Photocatalytic/adsorptive removal of methylene blue dye by electrophoretic nanostructured TiO2/montmorillonite composite films. J Adv Oxid Technol 16(2):292–297. https://doi.org/10.1515/jaots-2013-0211

Rauf M, Ashraf SS (2009) Fundamental principles and application of heterogeneous photocatalytic degradation of dyes in solution. Chem Eng J 151(1–3):10–18. https://doi.org/10.1016/j.cej.2009.02.026

Rodríguez JL, Pola F, Valenzuela MA, Poznyak T (2010) Photocatalytic deposition of nickel nanoparticles on titanium dioxide. MRS Online Proceedings Library Archive 1279. https://doi.org/10.1557/PROC-1279-53

Romero A, Dodorado F, Asencio I, García PB, Valverde JL (2006) Ti-pillared clays: synthesis and general characterization. Clay Clay Miner 54(6):737–747. https://doi.org/10.1346/CCMN.2006.0540608

Rossetto E, Petkowicz DI, dos Santos JH, Pergher SB, Penha FG (2010) Bentonites impregnated with TiO2 for photodegradation of methylene blue. Appl Clay Sci 48(4):602–606. https://doi.org/10.1346/CCMN.2006.0540608

Rutherford DW, Chiou CT, Eberl DD (1997) Effects of exchanged cation on the microporosity of montmorillonite. Clay Clay Miner 45(4):534–543. https://doi.org/10.1346/CCMN.1997.0450405

Ruvarac-Bugarčić IA, Šaponjić ZV, Zec S, Rajh T, Nedeljković JM (2005) Photocatalytic reduction of cadmium on TiO2 nanoparticles modified with amino acids. Chem Phys Lett 407(1–3):110–113. https://doi.org/10.1016/j.cplett.2005.03.058

Sahel K, Bouhent M, Belkhadem F, Ferchichi M, Dappozze F, Guillard C, Figueras F (2014) Photocatalytic degradation of anionic and cationic dyes over TiO2 P25, and Ti-pillared clays and ag-doped Ti-pillared clays. Appl Clay Sci 95:205–210. https://doi.org/10.1016/j.clay.2014.04.014

Saien J, Ghamari F, Azizi A (2016) The role of counter-anions in photocatalytic reduction of Ni (II) with a trace amount of titania nanoparticles. J Iran Chem Soc 13(12):2247–2255. https://doi.org/10.1007/s1373

Shenvi SS, Isloor AM, Ismail A (2015) A review on RO membrane technology: developments and challenges. Desalination 368:10–26. https://doi.org/10.1016/j.desal.2014.12.042

Singh C, Chaudhary R (2013) Visible light induced photocatalytic reduction of metals (Cr, cu, Ni, and Zn) and its synergism with different pH, TiO2, and H2O2 doses in simulated wastewater. J Renew Sustain Energ 5(5):053102. https://doi.org/10.1063/1.4818899

Srikanth B, Goutham R, Narayan RB, Ramprasath A, Gopinath K, Sankaranarayanan A (2017) Recent advancements in supporting materials for immobilised photocatalytic applications in waste water treatment. J Environ Manag 200:60–78. https://doi.org/10.1016/j.jenvman.2017.05.063

Sun H, Peng T, Liu B, Xian H (2015) Effects of montmorillonite on phase transition and size of TiO2 nanoparticles in TiO2/montmorillonite nanocomposites. Appl Clay Sci 114:440–446. https://doi.org/10.1016/j.clay.2015.06.026

Tahir M, Amin NS (2013) Photocatalytic reduction of carbon dioxide with water vapors over montmorillonite modified TiO2 nanocomposites. Appl Catal B Environ 142:512–522. https://doi.org/10.1016/j.apcatb.2013.05.054

Tan T, Beydoun D, Amal R (2003) Effects of organic hole scavengers on the photocatalytic reduction of selenium anions. J Photochem Photobiol A Chem 159(3):273–280. https://doi.org/10.1016/S1010-6030(03)00171-0

Testa JJ, Grela MA, Litter MI (2001) Experimental evidence in favor of an initial one-electron-transfer process in the heterogeneous photocatalytic reduction of chromium (VI) over TiO2. Langmuir 17(12):3515–3517. https://doi.org/10.1021/la010100y

Testa JJ, Grela MA, Litter MI (2004) Heterogeneous photocatalytic reduction of chromium (VI) over TiO2 particles in the presence of oxalate: involvement of Cr (V) species. Environ Sci Technol 38(5):1589–1594. https://doi.org/10.1016/j.apcatb.2006.09.002

Vicente, M., A. Gil and F. Bergaya (2013). Pillared clays and clay minerals. Dev Clay Sci, Elsevier. 5**:** 523–557https://doi.org/10.1016/B978-0-08-098258-8.00017-1

Volzone C, Rinaldi J, Ortiga J (2002) N2 and CO2 adsorption by TMA-and HDP-Montmorillonites. Mater Res 5(4):475–479. https://doi.org/10.1590/S1516-14392002000400013

Wang B, Zhang G, Sun Z, Zheng S (2014) Synthesis of natural porous minerals supported TiO2 nanoparticles and their photocatalytic performance towards Rhodamine B degradation. Powder Technol 262:1–8. https://doi.org/10.1016/j.powtec.2014.04.050

Wang Z, Xu Q, Meng T, Ren T, Chen D (2015) Preparation and characterization of CdS/TiO2–Mt composites with enhanced visible light Photocatalytic activity. Energy Environ Focus 4(2):149–156. https://doi.org/10.1166/eef.2015.1150

Wang Z, Liang H, Liao L, Chen L, Li Z, Feng J (2018) Zeolite supported-Nano TiO2 composites prepared by a facile solid diffusion process as high performance Photocatalysts. J Nanosci Nanotechnol 18(8):5726–5730. https://doi.org/10.1166/jnn.2018.15403

Waqas M, Wei Y, Mao D, Qi J, Yang Y, Wang B, Wang D (2017) Multi-shelled TiO2/Fe2TiO5 heterostructured hollow microspheres for enhanced solar water oxidation. Nano Res 10(11):3920–3928. https://doi.org/10.1007/s12274-017-1606-3

Williams G, Seger B, Kamat PV (2008) TiO2-graphene nanocomposites. UV-assisted photocatalytic reduction of graphene oxide. ACS Nano 2(7):1487–1491. https://doi.org/10.1021/nn800251f

Yahiro H, Miyamoto T, Watanabe N, Yamaura H (2007) Photocatalytic partial oxidation of α-methylstyrene over TiO2 supported on zeolites. Catal Today 120(2):158–162. https://doi.org/10.1016/j.cattod.2006.07.039

Yang C-S, Wang Y-J, Shih M-S, Chang Y-T, Hon C-C (2009) Photocatalytic performance of alumina-incorporated titania composite nanoparticles: surface area and crystallinity. Appl Catal A Gen 364(1–2):182–190. https://doi.org/10.1016/j.apcata.2009.05.052

Yang S, Liang G, Gu A, Mao H (2013) Synthesis of TiO2 pillared montmorillonite with ordered interlayer mesoporous structure and high photocatalytic activity by an intra-gallery templating method. Mater Res Bull 48(10):3948–3954. https://doi.org/10.1016/j.materresbull.2013.06.019

Yang C, Zhu Y, Wang J, Li Z, Su X, Niu C (2015) Hydrothermal synthesis of TiO2–WO3–bentonite composites: conventional versus ultrasonic pretreatments and their adsorption of methylene blue. Appl Clay Sci 105:243–251. https://doi.org/10.1016/j.clay.2015.01.002

Yariv S (2002) Introduction to organo-clay complexes and interactions. Marcel Dekker, New York

Yu Y, Wang J, Parr JF (2012) Preparation and properties of TiO2/fumed silica composite photocatalytic materials. Procedia Eng 27:448–456. https://doi.org/10.1016/j.proeng.2011.12.473

Yuan L, Huang D, Guo W, Yang Q, Yu J (2011) TiO2/montmorillonite nanocomposite for removal of organic pollutant. Appl Clay Sci 53(2):272–278. https://doi.org/10.4172/2161-0444.1000347

Zhang W, Zou L, Wang L (2009) Photocatalytic TiO2/adsorbent nanocomposites prepared via wet chemical impregnation for wastewater treatment: a review. Appl Catal A Gen 371(1–2):1–9. https://doi.org/10.1016/j.apcata.2009.09.038

Zhang T, Luo Y, Jia B, Li Y, Yuan L, Yu J (2015) Immobilization of self-assembled pre-dispersed nano-TiO2 onto montmorillonite and its photocatalytic activity. J Environ Sci 32:108–117. https://doi.org/10.1016/j.jes.2015.01.010. Epub 2015 Apr 24

Zhang Y, Sivakumar M, Yang S, Enever K, Ramezanianpour M (2018) Application of solar energy in water treatment processes: a review. Desalination 428:116–145. https://doi.org/10.1016/j.desal.2017.11.020

ZHENG Y, Zhiming P, Xinchen W (2013) Advances in photocatalysis in China. Chin J Catal 34(3):524–535. https://doi.org/10.1016/S1872-2067(12)60548-8

Zhou F-s, Chen D-m, Cui B-l, Wang W-h (2014) Synthesis and characterization of CdS/TiO2-Montmorillonite Nanocomposite with enhanced visible-light absorption. J Spectrosc 2014:1. https://doi.org/10.1155/2014/961230

Zou L, Luo Y, Hooper M, Hu E (2006) Removal of VOCs by photocatalysis process using adsorption enhanced TiO2–SiO2 catalyst. Chem Eng Process Process Intensif 45(11):959–964. https://doi.org/10.1016/j.cep.2006.01.014